

Light scattering by single erythrocyte: Comparison of different methods

Thomas Wriedt^{a,*}, Jens Hellmers^b, Elena Eremina^b, Roman Schuh^a

^a*Institut für Werkstofftechnik, Badgasteiner Str. 3, 28359 Bremen, Germany*

^b*Universität Bremen, Badgasteiner Str. 3, 28359 Bremen, Germany*

Abstract

In this paper we investigate the capabilities of different light scattering programs for light scattering simulation of the single human red blood cell, also known as erythrocyte. Knowledge of the scattering properties can help to solve the inverse problem of classifying erythrocytes according to size and shape using measured scattering diagrams. We compare the different programs by presenting the corresponding scattering diagrams. Then we give an overview of computation times and point out the different characteristics of the methods.

© 2005 Elsevier Ltd. All rights reserved.

Keywords: Erythrocyte; Electromagnetic scattering; Discrete sources method; Discrete dipole approximation; Multiple multipole program; Finite integration technique; T-matrix

1. Introduction

In recent years there has been an increased interest in light scattering by the human red blood cell, also known as erythrocyte. For experimental studies the scanning flow cytometer (SFC) can be used to measure the light scattering pattern of individual cells [1]. Knowledge about the theoretical light scattering behavior promises to enable advanced analysis of human blood, e.g. to detect abnormal mutated erythrocytes caused by disease. For this fast theoretical light scattering simulations are needed. Because of the special shape of the red blood cell and its size there are not many light scattering programs which are suitable.

In literature so far one can find several publications regarding to light scattering by the erythrocyte.

Lu et al. [2] for example used the finite difference time domain (FDTD), which is a time domain method like the finite integration technique (FIT) presented in this paper. Investigations using the discrete dipole approximation (DDA) were done by Karlsson et al. [3] and Yurkin et al. [4]. Eremina et al. [5] simulated light scattering by the erythrocyte using the discrete sources method (DSM). Nilsson et al. [6] used the T-matrix method. A boundary element method (BEM) approach can be found in Tsinopoulos et al. [7].

Although there is a number of publications about light scattering by erythrocyte they usually concentrate on one simulation method only. So the question for the most suitable method is still open.

*Corresponding author. Tel.: +49 421 2182507; fax: +49 421 2185378.

E-mail address: thw@iwt.uni-bremen.de (T. Wriedt).

In this paper we would like to give an overview of several theories and algorithms which we will compare than presenting computational results. As these methods for simulating light scattering are always strongly connected with the way how the shape of the cell is described, we start with a presentation of different approaches to model the human red blood cell. Then we give a short introduction into the following light scattering theories: DDA, FIT, DSM and Multiple Multipole Program (MMP). Additionally, we have a look at the latest developments of the Nullfield Method with Discrete Sources (NFM-DS). For the comparison we will present the corresponding light scattering diagrams for a single erythrocyte and also computation times. As every scattering theory has its own advantages and disadvantages, we will point out this in more detail. Finally, we would like to summarize our findings about accuracy, computational speed and characteristics of each method.

2. Erythrocyte

The erythrocyte is composed of hemoglobin, water and membrane components. As it does not contain any nucleus and thus no internal structure it provides a good opportunity to apply different computational light scattering methods. Nevertheless, the calculation of light scattering by the erythrocyte is not a trivial task, mostly due to the special cell characteristics: size, aspect ratio and a biconcave form.

In general, it can be described as a biconcave oblate disc with an average diameter between 6 and 8 μm while the average aspect ratio is up to 4 : 1 [1,8]—see also Fig. 1.

The refractive index also varies, depending on the incident wavelength and the surrounding media. For an incident wavelength of $\lambda = 632.8\text{ nm}$, the absolute index of refraction falls between 1.40 and 1.42, the imaginary part is usually neglected for this wavelength. For the relative refractive index 1.058 is usually used [8].

The main characteristic of the erythrocytes' shape is the presence of concavities on its sides. This makes an exact light scattering calculation especially difficult. To overcome this problem some studies use simplified shape models like flat cylinders with a rounded edge or oblate spheroids. Such approximations for example are

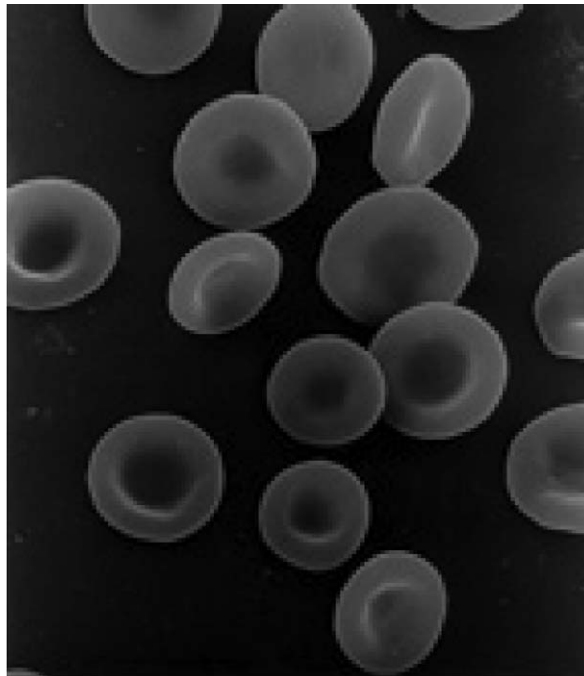


Fig. 1. Erythrocytes. Photo is courtesy of Drs. Noguchi, Rodgers, and Schechter of NIDDK. Public domain, taken from Wikipedia [9].

used when light scattering is simulated by the standard T-matrix approach [6]. The problem of shape models' influence has recently been investigated by Eremina et al. [5].

To construct a biconcave shape sometimes Cassini ovals are used [10,11]. These two-dimensional curves are characterized in such a way that the product of the distance of two fixed focal points is constant (while for a normal ellipse the sum of the distance of two fixed focal points is constant). By rotating such a curve around its vertical axis one can get a three-dimensional particle in the shape of an biconcave oblate disc.

The Cassini ovals have the Cartesian equation:

$$[(x - a)^2 + z^2][(x + a)^2 + z^2] = b^4, \quad (1)$$

which means

$$z^2 = \pm c(-a^2 - x^2 \pm (4x^2a^2 + b^4)^{1/2}), \quad (2)$$

respectively. The factor c is introduced to enable a direct variation of the overall thickness of the shape. The Cassini shape therefore depends on the relation b/a . If $a < b$ the curve is an oval loop, for $a = b$ the result is a lemniscate (like the ∞ -symbol) and for $a > b$ the curve consists of two separate loops. If a is chosen slightly smaller than b one gets a concave, bone-like shape. This concavity will get deeper the closer a gets to b .

For most of our light scattering simulations presented in this paper we use the equation given by Skalak et al. [8,12]:

$$z^2 = (0.86d/2)^2[1 - (2x/d)^2][0.01384083 + 0.2842917(2x/d)^2 + 0.01306932(2x/d)^4], \quad (3)$$

where d is the diameter.

A visualization of this shape obtained from the *Hyperfun* software [13] is presented in Fig. 2.

To give an impression of the different resulting shapes, Fig. 3 shows the profiles of (2) and (3). The Cassini shape model is adjusted to a diameter of $6.3 \mu\text{m}$, the resulting aspect ratio is $\approx 4 : 1$. This can be reached by choosing $a = 2.2$, $b = 2.25$, $c = 0.66$. In both cases main and minimum (concavity) thicknesses are congruent. One can see that the Cassini oval has a smaller concavity with a steep curve and a more pointy edge compared to the Skalak shape.

Another equation to describe the erythrocyte shape was introduced by Fung [14]. This general shape description is given by

$$z = (1 - (2x/d)^2)^{1/2} (c_1 + c_2(2x/d)^2 + c_3(2x/d)^4), \quad (4)$$

$c_1 - c_3$ are constants which have to be determined for the specific shape and d denotes the overall diameter of the erythrocyte.

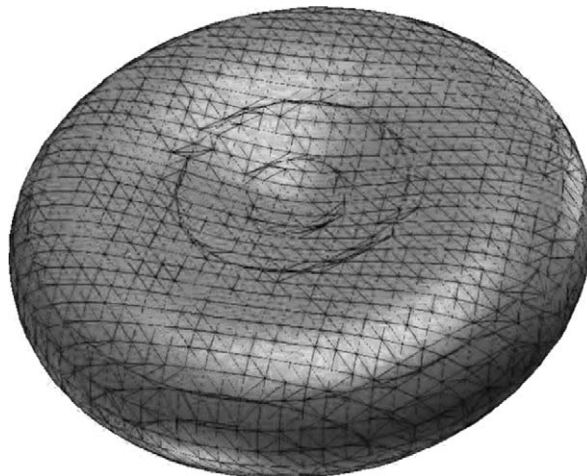


Fig. 2. Shape of an erythrocyte described by (3). The diameter d is $6.3 \mu\text{m}$.

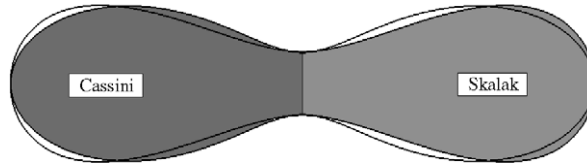


Fig. 3. Comparison of different shape models: Skalak (3) and Cassini (2). The diameter d is $6.3\mu\text{m}$, the Cassini parameters are $a = 2.2$, $b = 2.25$, $c = 0.66$.

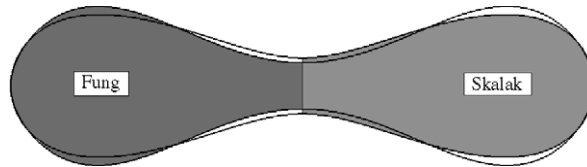


Fig. 4. Comparison of different shape models: Skalak (3) and Fung (5). The diameter d is $7.6\mu\text{m}$, the parameter $\varepsilon = 0.26$.

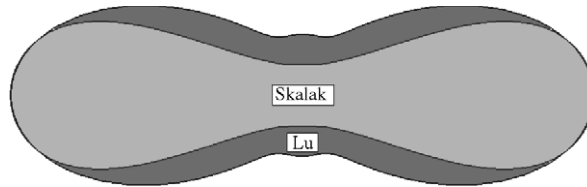


Fig. 5. Comparison of different shape models: Skalak (3) and Lu (6). The diameter d is $7.5\mu\text{m}$, $q = 5$, $a = 3$ and $b = 0.75$.

Yurkin et al. [4] use this equation with the following parameters:

$$z = \varepsilon d(1 - (2x/d)^2)^{1/2} (0.1583 + 1.5262(2x/d)^2 - 0.8579(2x/d)^4), \tag{5}$$

where ε enables to manipulate the aspect ratio directly.

Fig. 4 shows the differences in the resulting shapes. For the same diameter, the equation of Fung leads to a greater distance between maximum and minimum (concavity) thickness.

Another approach is given by Lu [2]. Here, the shape is described by

$$r = a \sin^q(\theta) + b, \tag{6}$$

with $q = 5$, $a = 3$ and $b = 0.75$. With these parameters the resulting diameter is $\approx 7.5\mu\text{m}$. Compared to Skalak (3), the concavity has a smaller diameter and a different shape, additionally the aspect ratio of 3.4 : 1 is lower—see Fig. 5.

3. Light scattering theories

In this section we would like to give a short overview of the theoretical approaches that we use for our scattering computations. This overview gives the basic ideas and concepts of the different theories. Additionally, we will show a graphical illustration of the particle shape model that was used for the corresponding program. A review of several light scattering methods can be found in the articles of Wriedt [15,16] and Kahnert [17]. A collection of programs is available in the Internet on the webpages of Wriedt [18] and Flatau [19].

In principle, the used programs can be divided into two categories; surface-based and volume-based programs.

For the volume-based programs we used

- DDA,
- FIT

and for the surface-based ones we used

- DSM,
- MMP,
- NFM-DS.

In general, volume-based programs have the advantage that they are capable of simulating light scattering by all kind of particle shapes. On the other side for this it is necessary to discretize the whole particle volume—and sometimes even part of the surrounding medium. This leads to high computational efforts and corresponding long computation times. Surface-based programs usually are much faster, especially when they can make use of rotational symmetry properties. Unfortunately, they might be restricted to more simple particle shapes. More details to this will be given in the following subsections.

3.1. Discrete dipole approximation

The DDA was developed by Purcell and Pennypacker in 1973 [20]. This method is used in many different fields of light scattering investigation, mainly because the popular program *DDSCAT* by Draine [21] is freely available.

It is a volume integral equation method where the scatterer is approximated by lattice of dipoles—see Fig. 6. The spacing between these dipoles has to be small compared to the wavelength; the number of dipoles depends on the required numerical accuracy, the geometry of the particle and the refractive index. The dipoles have an oscillating polarization in response to both the incident plane wave and the electric fields due to all the other dipoles in the array. The far field results from the superposition of the fields of all dipoles. For our computations, we use the program *DDSCAT* by Draine.

3.2. Finite integration technique

The FIT originates in the developments by Weiland [22]. The method provides a discrete reformulation of Maxwell's equations in their integral form. It restricts the electromagnetic field problem with its open boundary problem to a simply connected and bounded space containing the region of interest—see Fig. 7. This computational domain then is decomposed into a finite number of volume elements; the result is a grid of cells. In a cartesian grid, the algorithm of the FIT is similar to the FDTD. Then electric and magnetic characteristics on the volume elements are examined. One problem is the stair case approximation, additionally an absorbing boundary is required to terminate the computational domain without reflection. To compute the far-field scattering diagrams a near to far field transformation is needed.

Here, we use *CST Microwave Studio* [23] as software for light scattering simulation, see also Fig. 7.

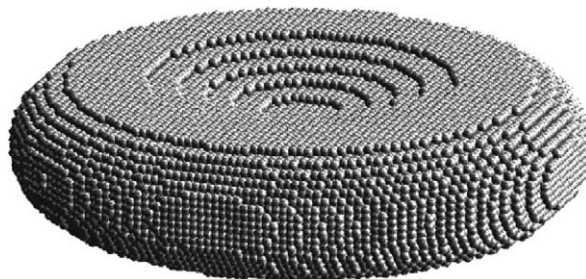


Fig. 6. Erythrocyte shape model as used for the DDA simulation.

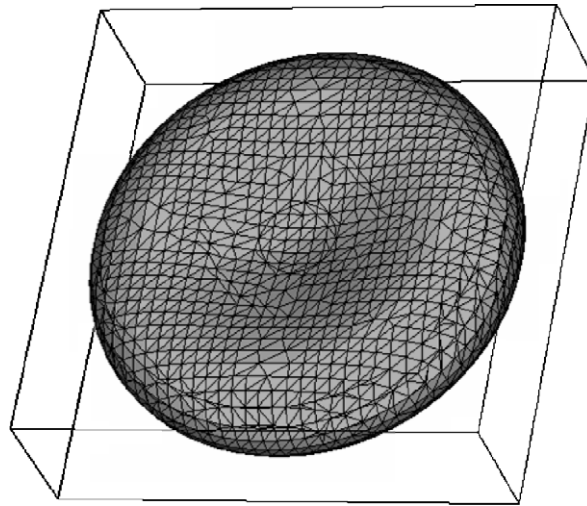


Fig. 7. Erythrocyte shape model as used for the FIT simulation with CST Microwave Studio. Note that here the surrounding media has to be discretized too—symbolized by the outer rectangular grid-box.

3.3. Discrete sources method

Originally, the theoretical principles of the DSM were established about 40 years ago independently by Kupradze [24] in the Soviet Union and Yasuura [25] in Japan. The first version of the DSM was published in 1980 by Sveshnicov and Eremin [26]. Since then several research groups have been working on this worldwide. Recently, the method was modified for light scattering by a wide variety of objects, from long fibers [27] to oblate spheroids and concave particles [5]. Also evanescent scattering [28] can be calculated. The DSM is a semi-analytical method. A mathematical statement of the light scattering problem in a frame of DSM consists of Maxwell equations, transmission conditions at the interface and obstacle boundary and infinity conditions to provide the unique solution. An approximate solution is constructed as a linear combination of fields of discrete sources (multipoles or dipoles deposited in a supplementary domain) with certain amplitudes so that it satisfies all the conditions of a boundary value scattering problem except the boundary conditions on a obstacle surface. The last condition is used to determine the amplitudes of discrete sources using a generalized point matching scheme. Contrary to other methods DSM has the advantage that it allows to estimate an a posteriori error by calculating the surface residual on the obstacle boundary and efficiently makes use of axial symmetry of the scatterer. In this way computational time is reduced.

A comprehensive overview of the DSM can be found in the book of Eremin et al. [29].

Usually the discrete sources are placed on the axis of symmetry. As this is not suitable for an oblate scatterer in this case the sources are arranged in a complex plane—see Fig. 8.

3.4. Multiple multipole program

The MMP was introduced by Hafner and Bomholt in the early nineties [30]. It is a variant of the generalized multipole techniques (GMT) [31]. Here, electromagnetic fields are expressed as a linear combination of multiple multipoles, which are located inside the obstacle for the scattered fields, while they are distributed in the exterior domain for the internal fields; both according to the shape of the domain. The amplitudes of the multipoles are obtained by enforcing the boundary conditions in a set of matching points by applying generalized point matching. In this way it is a semi-analytical method.

Practically, the computational algorithm uses an approximate solution that finally converges to the exact one. The corresponding expansion coefficients can be calculated by a least-square approach.

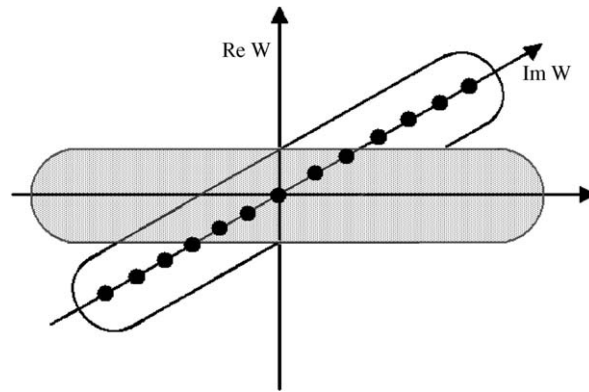


Fig. 8. Sketch to demonstrate the concept of discrete sources in a complex plane.

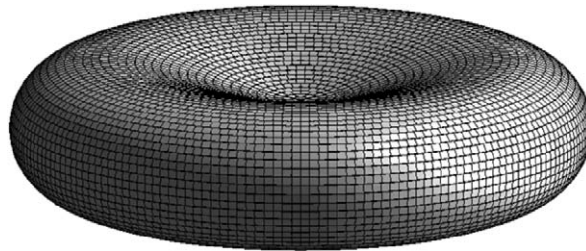


Fig. 9. Erythrocyte shape model as used for the MMP simulation.

Because the origin of multipoles can be set flexibly, the MMP is able to calculate scattering by arbitrary shaped particles. For the shape model we used see Fig. 9.

3.5. Nullfield Method with discrete sources

The NFM-DS is still in progress development by Doicu and Wriedt [32–34]. The theory is based on the Nullfield Method [35], which in its standard form is considered hardly capable of calculating light scattering by shapes with large sizes or aspect ratios [36]. The additional presence of concavities makes this even more problematic [3,37]. Extending the Nullfield Method by the use of discrete sources now enables to calculate light scattering by prolate particles with high aspect ratios [38]. By situating the discrete sources in a complex plane (see Fig. 8) light scattering by oblate particles of large sizes and aspect ratios can be calculated [39]; also biconcave particles can be simulated now [40].

In principle, the scatterer is replaced by a set of surface currents so that in the exterior region the sources and fields are exactly the same as those existing in the original scattering problem. Then the total electric field is expanded in terms of spherical vector wave functions. For an axially symmetrical scatterer, it is possible to reduce the problem of surface approximation to a sequence of one-dimensional problems relative to Fourier harmonics of the surface currents by using a system of multipoles—the discrete sources—and by expanding the external excitation in Fourier series.

The biggest advantage of this method is that it enables to calculate the T-matrix, which contains all information about the scattering process.

In our case investigations so far concentrate on smaller biconcave particle shapes based on Cassini ovals.

4. Results

In this section we would like to present some light scattering simulation results for a single erythrocyte.

For this we start with light scattering diagrams calculated by the different methods with the exception of the NFM-DS, which is treated separately.

This comparison would not be complete without final remarks on the typical characteristics of the different algorithms—like computation time and limits of additional investigations. So an overview of these qualities is given, too.

4.1. Scattering diagrams for DSM, MMP, FIT and DDA

We start with a comparison between DSM, MMP and FIT. To describe the erythrocyte particle shape, we use the formula by Skalak (3) with a diameter d of $6.3\ \mu\text{m}$. As incident wavelength we choose $\lambda = 632.8\ \text{nm}$, the corresponding refractive index is 1.42. Of course the intensity of scattered light also depends on the orientation of the particle. As the main aim of this work is to compare the different computational methods, light scattering is calculated for incident light parallel to the vertical (rotational) axis of the erythrocyte as this leads to the most significant scattering diagrams.

Fig. 10 shows the scattering diagrams for p- and s-polarization. As one can see there is a very good congruence between the results of the different programs.

In Fig. 11 the same results are presented in a linear scale for the scattering angle range between 10° and 50° . This range is of special interest as it is covered by most experimental devices [1]. Even in this detailed presentation without a logscale y-axis, the simulation results correspond well.

The diagrams in Fig. 12 compare DSM results to those by DDA; the same particle shape with the same wavelength and refraction index is used. Again we get a very good congruence between the different methods—also in the range between 10° and 50° —see Fig. 13.

4.2. NFM-DS

As mentioned above the NFM-DS is still under development. For oblate discs without concavities, it was shown that this method is able to calculate light scattering by particles with a diameter and aspect ratio in the area of typical erythrocytes without problems [39]; even bigger size parameters and aspect ratios are possible. Recent work also proved that this method is capable of calculating light scattering by biconcave particles based on Cassini ovals [40]. So far this is restricted to biconcave particles with lower size parameters as there are still numerical problems with size parameters in the range of the erythrocyte.

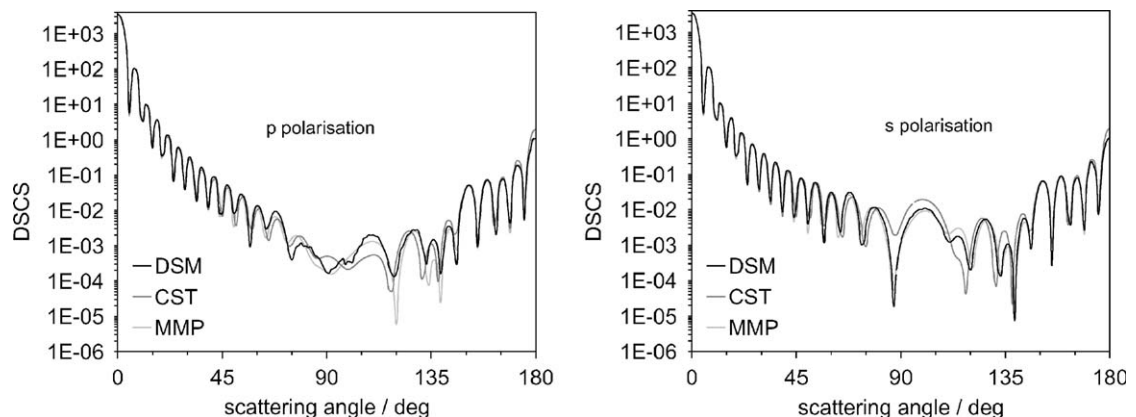


Fig. 10. Comparison of light scattering results between DSM, CST and MMP; p- and s-polarized. The shape is based on Skalak's formula; the diameter is $6.3\ \mu\text{m}$. The direction of incident light is parallel to the rotational axis. $\lambda = 632.8\ \text{nm}$, the refractive index is 1.42.

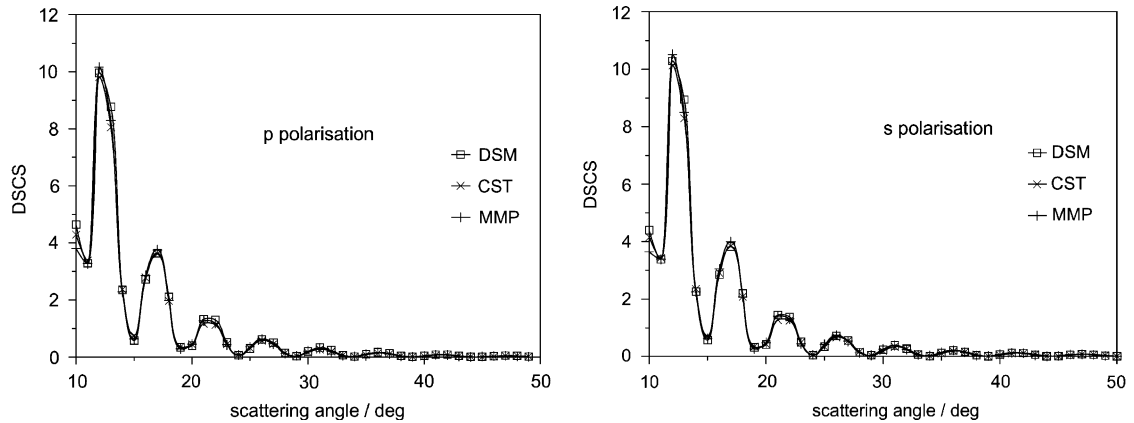


Fig. 11. More detailed comparison of light scattering results in the area of $10\text{--}50^\circ$ between DSM, CST and MMP; p- and s-polarized. The shape is based on Skalak's formula; the diameter is $6.3\ \mu\text{m}$. The direction of incident light is parallel to the rotational axis. $\lambda = 632.8\ \text{nm}$, the refractive index is 1.42.

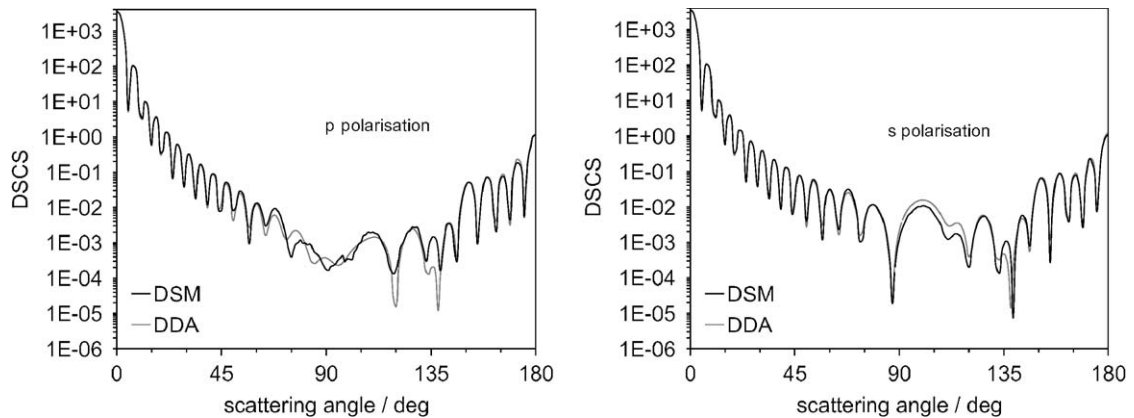


Fig. 12. Comparison of light scattering results between DSM and DDA; p- and s-polarized. The shape is based on Skalak's formula; the diameter is $6.3\ \mu\text{m}$. The direction of incident light is parallel to the rotational axis. $\lambda = 632.8\ \text{nm}$, the refractive index is 1.42.

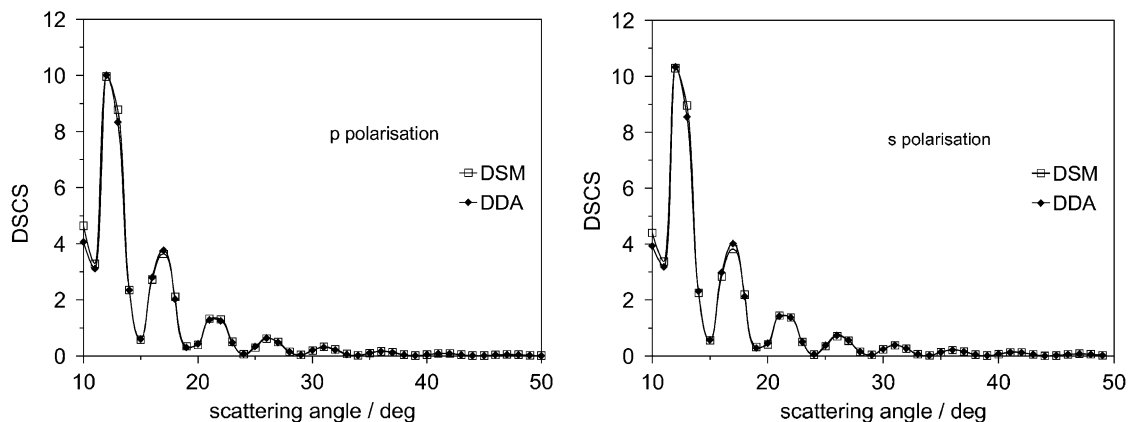


Fig. 13. More detailed comparison of light scattering results in the area of $10\text{--}50^\circ$ between DSM and DDA; p- and s-polarized. The shape is based on Skalak's formula; the diameter is $6.3\ \mu\text{m}$. The direction of incident light is parallel to the rotational axis. $\lambda = 632.8\ \text{nm}$, the refractive index is 1.42.

To cope with this, actual investigations are concentrating on the influence of the arrangement of the discrete sources as well as number, size and arrangement of the surface elements which are used as integration areas. Results so far are promising, so that light scattering calculation by the NFM-DS for full size erythrocytes should be possible in the near future. This would bring reasonable advantages: as the T-matrix is calculated, additional investigations like varying the direction of the incident light, the use of a Gaussian beam instead of a plane wave as incident light or orientation averaging could be done with low computational efforts.

In this paper we would like to present what at least can be calculated in the present time. Fig. 14 shows the scattering diagrams for a Cassini oval-based particle like in Fig. 3 for a diameter of $3.15\ \mu\text{m}$ —so half the diameter which was used so far in the Skalak term. We compare the NFM-DS with the DSM. The wavelength is $\lambda = 632.8\ \text{nm}$ and the refractive index is 1.42.

One can see that for this particle size, the NFM-DS is capable of calculating light scattering, which is a remarkable advancement over the conventional T-matrix methods.

As soon as the T-matrix is calculated, further investigations can be done with low computational efforts. Therefore Fig. 15 shows the scattering diagram for an angle $\theta = 30^\circ$ between the direction of the incident light and the rotational axis. Again we get a very good congruence between DSM and NFM-DS results.

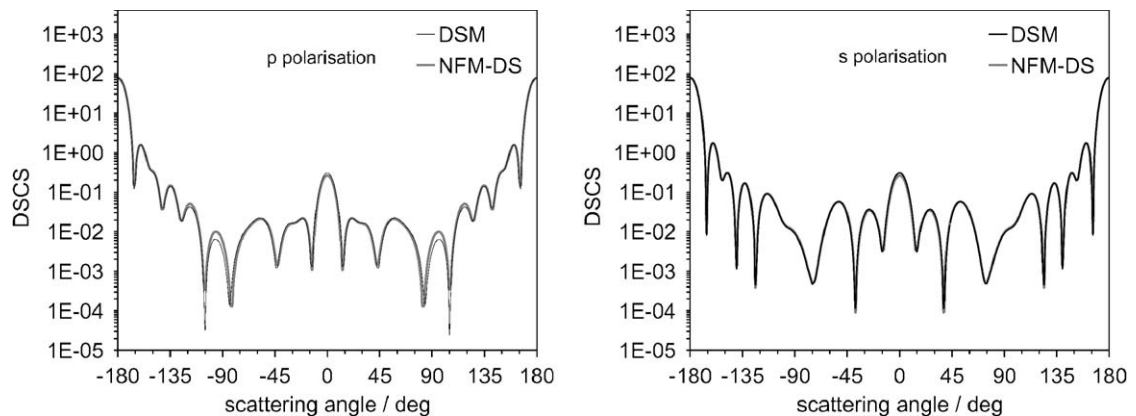


Fig. 14. Comparison of light scattering results between DSM and NFM-DS; p- and s-polarized. The shape is based on a Cassini oval with parameters $a = 1.1$, $b = 1.125$, $c = 0.66$; the diameter is $3.15\ \mu\text{m}$. The direction of incident light is parallel to the rotational axis. $\lambda = 632.8\ \text{nm}$, the refractive index is 1.42.

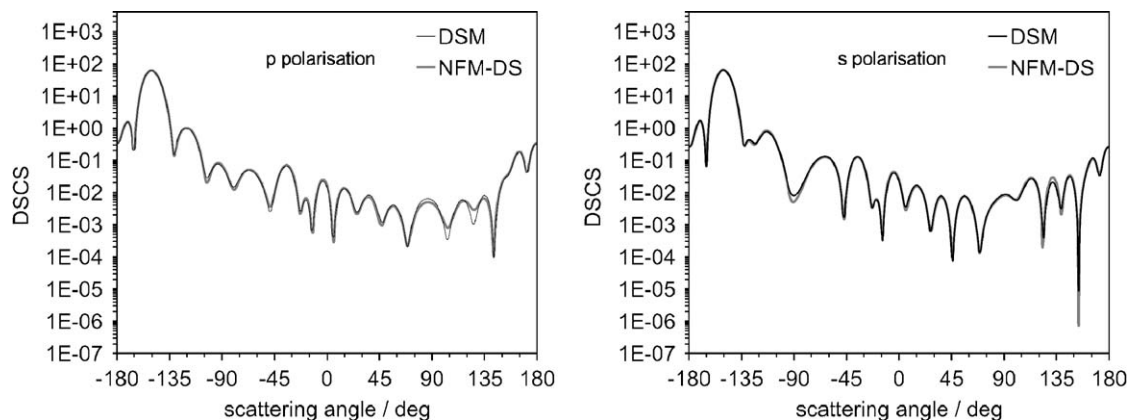


Fig. 15. Comparison of light scattering results between DSM and NFM-DS; p- and s-polarized. The shape is based on a Cassini oval with parameters $a = 1.1$, $b = 1.125$, $c = 0.66$; the diameter is $3.15\ \mu\text{m}$. The angle between incident light and rotational axis is 30° . $\lambda = 632.8\ \text{nm}$, the refractive index is 1.42.

Table 1
Estimation for computation times

Program	Shape	Discretization	Precision	Time
DSM	Rot. sym.		Double + quad	5 min
MMP	Mirror sym.		Quad	1 h
DDA	3D	$11/\lambda$	Double	1 h
FIT (<i>CST</i>)	3D	$25/\lambda$		7 h

All computations were done on a PC, Pentium 4 3000 MHz.

4.3. Computation times, additional computations, general remarks

The presented scattering diagrams show that all methods deliver nearly the same results. Nevertheless there are differences, which have to be considered—especially for the user. For example, DDA is very flexible regarding to the particle shape. But as the whole volume of the particle has to be discretized it needs a lot of computational efforts. DSM on the other side is restricted to rotational symmetrical particles, but it is very fast. To give an impression we would like to present an overview of the observed computation times. As the different programs used offer different features which can have influence on the computation time, this overview can only be an estimation; a direct comparison is difficult to achieve. Nevertheless some trends are obvious and should be mentioned. Table 1 shows the computation times we measured for our calculations.

These observations show that DSM is by far the fastest method. This is a big advantage that even increases if one considers that the method is capable of calculating all the light scattering diagrams for multiple directions of incident light at once—while for example with DDA one has to start (the already more time consuming) simulation from the beginning again for every single incident angle. This has to be considered when choosing an appropriate method for calculating light scattering diagrams.

So a ranking of computational speeds would set DSM first, followed by MMP slightly ahead of DDA. The FIT using program *CST* needs much longer than the other algorithms because a high discretization has to be used to achieve reasonable results; but there might be possibilities for optimization.

The NFM-DS is left out as it is not capable of calculating the full size erythrocyte so far. Nevertheless we would like to give some general remarks. The program suffers strongly from the need of using quad precision when calculating extreme particle shapes. This numerical accuracy is necessary to achieve converging results [41]. So the first calculation of the T-matrix is a time-consuming process. As soon as the T-matrix is calculated things change. Light scattering diagrams can be calculated even faster than by DSM.

5. Summary and conclusions

The presented diagrams show that DDA, FIT, DSM and MMP deliver reasonable results when investigating light scattering by a single erythrocyte. So one can choose from a broad range of methods with a couple of algorithms. Nevertheless some of the programs are more suitable than others.

The most advantageous is DSM. It combines the fastest computational speed with the ability to calculate light scattering for any directions of incident light at once. But for this it requires rotational symmetry of the particle. If flexibility of the particle shape is needed DDA seems to be the best choice. As a volume-based algorithm it can handle all kinds of particle shapes. Because of this it is not that fast as DSM. Another problem is that DDA can only calculate a result for one direction of incident light at once; if light scattering diagrams for other directions are required, the calculation has to be redone.

The other algorithms in principle are acceptable alternatives for computations of light scattering by erythrocyte. From the characteristics MMP is close to DSM and FIT (*CST*) is close to DDA, but their computational speeds are much slower.

NFM-DS is promising but cannot be compared easily to the other methods. First of all more progress is needed to calculate full size erythrocytes. For computation times: the calculation of the T-matrix is a time-consuming process. But as soon as the T-matrix is calculated it allows by far the fastest calculation of scattering diagrams. So the usefulness of this method depends much on the specific problem that has to be investigated. Nevertheless it looks reasonable to improve this method further.

Acknowledgements

We would like to acknowledge support of this work by Deutsche Forschungsgemeinschaft DFG.

References

- [1] Maltsev VP, Semyanov KA. Characterisation of bio-particles from light scattering VSP. Utrecht, Boston; 2004.
- [2] Lu JQ, Yang P, Hu XH. Simulations of light scattering from a biconcave red blood cell using the finite-difference time-domain method. *J Biomed Opt* 2005;10(2):024022.
- [3] Karlsson A, He JP, Swartling J, Andersson-Engels S. Numerical simulations of light scattering by red blood cells. *IEEE Trans Biomed Eng* 2005;52(1).
- [4] Yurkin MA, Semyanov KA, Tarasov PA, Chernyshev AV, Hoekstra AG, Maltsev VP. Experimental and theoretical study of light scattering by individual mature red blood cells by use of scanning flow cytometry and a discrete dipole approximation. *Appl Opt* 2005;44(25):5249–56.
- [5] Eremina E, Eremin Y, Wriedt T. Analysis of light scattering by erythrocyte based on discrete sources method. *Opt Commun* 2005;244:15–23.
- [6] Nilsson AMK, Alsholm P, Karlsson A, Andersson-Engels S. T-matrix computations of light scattering by red blood cells. *Appl Opt* 1998;37:2735–48.
- [7] Tsinopoulos SV, Polyzos D. Scattering of He–Ne laser light by an average-sized red blood cell. *Appl Opt* 1999;38(25):5499–510.
- [8] Shvalov AN, Soini JT, Chernyshev AV, Tarasov PA, Soini E, Maltsev VP. Light-scattering properties of individual erythrocytes. *Appl Opt* 1999;38(1):230–5.
- [9] Wikipedia. URL: <<http://commons.wikimedia.org/wiki/Image:Redbloodcells.jpg>>.
- [10] Angelov B, Mladenov IM. On the geometry of red blood cell. Geometry, integrability and quantization. Varna: Bulgaria; 1999.
- [11] Mazon P, Muller S. Dielectric or absorbing particles: EM surface fields and scattering. *J Opt* 1998;29:68–77.
- [12] Skalak R, Tozeren A, Zarda RP, Chien S. Strain energy function of red blood cell membranes. *Biophys J* 1973;13:245–64.
- [13] HyperFun Project: Language and Software for F-rep Modeling. URL: <<http://www.hyperfun.org>>.
- [14] Fung YC, Tsang WC, Patitucci P. High-resolution data on the geometry of red blood cells. *Biorheology* 1981;18:369–85.
- [15] Wriedt T. A review of elastic light scattering theories. Part Syst Charact 1998;15:67–74.
- [16] Wriedt T, Comberg U. Comparison of computational scattering methods. *JQSRT* 1998;60:411–23.
- [17] Kahnert FM. Numerical methods in electromagnetic scattering theory. *JQSRT* 2003;79–80:775–824.
- [18] Wriedt T. Electromagnetic Scattering Programs. URL: <<http://www.t-matrix.de>>.
- [19] Flatau P. SCATTERLIB Light Scattering Codes Library. URL: <<http://atol.ucsd.edu/~pflatau/>>.
- [20] Purcell EM, Pennypacker CR. Scattering and absorption of light by nonspherical dielectric grains. *Astrophys J* 1973;186:705–14.
- [21] Draine BT, Flatau PJ. Discrete-dipole approximation for scattering calculations. *J Opt Soc Am A* 1994;11:1491–9.
- [22] Weiland T. A discretization method for the solution of Maxwell's equation for six-components fields. *Electron Commun AEU* 1977;31:116–20.
- [23] Computer Simulation Technology. URL: <<http://www.cst.com/>>.
- [24] Kupradze VD. About approximate solution of mathematical physics problems. *Usp Mat Nauk* 1967;22(2):59–107.
- [25] Okuno Y, Ikuno H. The Yasuura method for solving boundary problems for Helmholtz equation in uniform medium. *Radiotechn Electron* 1992;37:1744–63.
- [26] Sveshnicov AG, Eremin YA. Numerical investigation of scattering problems on bodies of revolution by non-orthogonal series method. *Izv Vyssh Uchebn Zaved Radiofiz* 1980;23(8):580.
- [27] Eremina E, Wriedt T. Review of light scattering by fiber particles with a high aspect ratio. *Recent Res Develop Opt* 2003;3:297–318.
- [28] Eremin YA, Wriedt T. Large dielectric particle in an evanescent wave field near a plane surface. *Opt Commun* 2002;214:39–45.
- [29] Eremin YA, Orlov N, Sveshnikov A. In: Wriedt T, editor. Models of electromagnetic scattering problems based on discrete sources method. Generalizes multipole techniques for electromagnetic and light scattering. Amsterdam: Elsevier; 1999. p. 39–80.
- [30] Hafner C, Bomholt L. The 3D electromagnetic wave simulator, 3D MMP software and user's guide. Chichester: Wiley; 1993.
- [31] Wriedt T, editor. Mechanics and mathematical methods—vol. 4: generalized multipole techniques for electromagnetic and light scattering. Amsterdam: Elsevier; 1999.
- [32] Doicu A, Eremin Y, Wriedt T. Acoustic and electromagnetic scattering analysis using discrete sources. San Diego: Academic Press; 2000.
- [33] Doicu A, Wriedt T. Extended boundary condition method with multipole sources located in the complex plane. *Opt Commun* 1997;139:85–98.

- [34] Doicu A, Wriedt T. Calculation of the T-matrix in the null-field method with discrete sources. *J Opt Soc Am A* 1999;16:2539–44.
- [35] Waterman PC. Matrix formulation of electromagnetic scattering. *Proc IEEE* 1965;53:805–12.
- [36] Mishchenko MI, Travis LD, Mackowski DW. T-matrix computations of light scattering by nonspherical particles: a review. *JQSRT* 1996;55:535–75.
- [37] Wiscombe WJ, Mugnai A. Single scattering from nonspherical Chebyshev particles: a compendium of calculations. *NASA Reference Publication*, vol. 1157. 1985.
- [38] Pulbere S, Wriedt T. Light scattering by cylindrical fibers with high aspect ratio using the null-field method with discrete sources. *Part Syst Charact* 2004;21:213–8.
- [39] Hellmers J, Wriedt T, Doicu A. Light scattering simulation by oblate discsphere using the Nullfield Method with discrete sources located in the complex plane. *J Mod Opt* 2005.
- [40] Hellmers J, Eremina E, Wriedt T. Simulation of light scattering by biconcave Cassini ovals using the Nullfield Method with discrete sources. *J Opt A* 2005.
- [41] Mishchenko MI, Travis LD. T-matrix computations of light scattering by large spheroidal particles. *Opt Commun* 1994;109:16–21.